CLINICAL AND VACCINE IMMUNOLOGY, July 2006, p. 768–778 Vol. 13, No. 7
1556-6811/06/$08.00+0 doi:10.1128/CVI.00042-06

Simian Immunodeficiency Virus (SIV)/Immunoglobulin G Immune Complexes in SIV-Infected Macaques Block Detection of CD16 but Not Cytolytic Activity of Natural Killer Cells

Qing Wei,[1] Jackie W. Stallworth,[1] Patricia J. Vance,[2] James A. Hoxie,[2] and Patricia N. Fultz[1]*

Department of Microbiology, University of Alabama at Birmingham, Birmingham, Alabama 35294,[1] *and Department of Medicine, University of Pennsylvania, Philadelphia, Pennsylvania 19104*[2]

Received 2 February 2006/Returned for modification 6 March 2006/Accepted 25 April 2006

Natural killer cells are components of the innate immune system that play an important role in eliminating viruses and malignant cells. Using simian immunodeficiency virus (SIV) infection of macaques as a model, flow cytometry revealed a gradual loss of $CD16^+$ NK cell numbers that was associated with disease progression. Of note, the apparent loss of NK cells was detected in whole-blood samples but not in isolated peripheral blood mononuclear cells (PBMC), suggesting that an inhibitor(s) of the antibody used to detect CD16, the low-affinity immunoglobulin G (IgG) receptor, was present in blood but was removed during PBMC isolation. (Actual decreases in $CD16^+$ cell numbers in PBMC generally were not detected until animals became lymphopenic.) The putative decrease in $CD16^+$ cell numbers in whole blood correlated with increasing SIV-specific antibody titers and levels of plasma virion RNA. With the addition of increasing amounts of plasma from progressor, but not nonprogressor, macaques to PBMC from an uninfected animal, the apparent percentage of $CD16^+$ cells and the mean fluorescence intensity of antibodies binding to CD16 declined proportionately. A similar decrease was observed with the addition of monomeric IgG (mIgG) and IgG immune complexes (IgG-ICs) purified from the inhibitory plasma samples; some of the ICs contained SIV $p27^{gag}$ antigen and/or virions. Of interest, addition of purified IgG/IgG-ICs to NK cell lytic assays did not inhibit killing of K562 cells. These results indicate that during progressive SIV and, by inference, human immunodeficiency virus disease, $CD16^+$ NK cell numbers can be underestimated, or the cells not detected at all, when one is using a whole-blood fluorescence-activated cell sorter assay and a fluorochrome-labeled antibody that can be blocked by mIgG or IgG-ICs. Although this blocking had no apparent effect on NK cell activity in vitro, the in vivo effects are unknown.

NK cells, which are cytotoxic for virus-infected and neoplastic cells, are important components of the innate immune system and facilitate the transition to adaptive, pathogen-specific responses (7, 11). In the latter function, NK cells interact with dendritic cells and secrete cytokines and chemokines to which T and B cells, as well as dendritic cells, respond (16, 28, 66). During human immunodeficiency virus (HIV) infection, consistent results with regard to the fate of NK cells and their ability to secrete cytokines and lyse target cells have not been obtained. In some studies, numbers of NK cells (or of a subset of NK cells) decreased in all stages of infection or were a function of disease progression; that is, changes were associated with low $CD4^+$ T-cell numbers and high viral burdens (3, 20, 47, 48, 65). Alternatively, expansion of dysfunctional subsets of NK cells has been reported (2, 33, 50), while in other studies there appeared to be no loss in NK cell numbers and/or in cytotoxic activity, either by direct lysis of target cells or in antibody-dependent cellular cytotoxicity (ADCC) (1, 35). For HIV-infected patients and simian immunodeficiency virus (SIV)-infected macaques, ADCC has been detected within days or a few weeks after symptomatic acute infection, appears to be important for the initial decrease in virus load during acute infections, and is associated with long-term stable disease (4, 5, 13, 25, 64). Likewise, the ability of NK cells from HIV-infected patients to secrete cytokines, such as gamma interferon (IFN-γ), RANTES, and macrophage inflammatory protein 1α and -1β (MIP-1α and -1β), that not only are required for adaptive immunity but also can inhibit HIV binding to CCR5 has been linked to delay in disease progression (6, 24, 40, 55). The fact that apparently uninfected but exposed intravenous drug users have high NK cell activity also suggests a role for NK cells in controlling or preventing primary infections (59). This suggestion is supported by findings in the SIV macaque model that vaccine-elicited ADCC was associated with lower viremia after mucosal challenge with pathogenic virus (30).

Although the majority of human NK cells are defined by expression of CD56 and CD16 on the cell surface, macaque NK cells preferentially express CD16, and only a small proportion (range, 5 to 20%) of these $CD16^+$ cells also express CD56 (9, 60, 68; Q. Wei and P. N. Fultz, unpublished data). Furthermore, a majority (range, 60 to 95%) of macaque $CD16^+$ NK cells are $CD8\alpha^+$; therefore, immunophenotypically most macaque NK cells are $CD16^+$ $CD8\alpha^+$ $CD3^-$ (major population) or $CD16^+$ $CD8\alpha^-$ $CD3^-$ (minor population) (9, 10, 15, 34, 60, 68). CD16 is the low-affinity immunoglobulin G (IgG) Fc receptor IIIa isoform (FcγRIIIa) and associates with homo- or heterodimers of CD3-associated ζ chain and FcεRIγ, signaling adaptors that are phosphorylated by $p56^{lck}$ after

* Corresponding author. Mailing address: Department of Microbiology, University of Alabama at Birmingham, BBRB 509E, 845 19th Street South, Birmingham, AL 35294. Phone: (205) 934-0790. Fax: (205) 975-6788. E-mail: pnf@uab.edu.

CD16 cross-linking (44, 45). Ligation of CD16 by monoclonal antibodies (MAbs) to CD16 or IgG immune complexes (IgG-ICs) and recognition of Fc fragments bound to cell surface antigens can lead to activation, cytokine secretion, cytotoxicity, and/or proliferation of NK cells (67); however, CD16 ligation on cytokine-activated NK cells results in apoptosis (56). CD16 preferentially recognizes IgG bound to antigen, but CD16 recognition and binding of soluble monomeric IgG (mIgG) can occur in vivo, is labile, and can inhibit NK cell activity (23, 61, 62). Although circulating ICs containing HIV have been detected in serum and plasma samples from infected persons (52, 54), the exact impact of ICs on the various subsets of NK cells has not been defined.

The pathogenesis of SIVmac239, an infectious molecular clone, is well defined: it causes AIDS in various macaque species (*Macaca* spp.) within approximately 6 months to 2 years after inoculation (26, 39). To understand the roles in pathogenesis of the various proteins encoded by SIV/HIV, this model system has been used extensively (18). In an earlier study to evaluate the effect of mutation of a conserved tyrosine (Y721) that is part of a sorting and endocytosis signal (YRPV) in the cytoplasmic tail of the SIVmac239 Env glycoprotein, we showed that rhesus macaques inoculated with SIVmac239 containing a tyrosine 721-to-isoleucine mutation (SIVmac239-Y/I) or a deletion of Y721 and the preceding glycine (SIVmac239ΔGY) had low to undetectable viral burdens, stable numbers of $CD4^+$ lymphocytes, and no clinical signs of disease—that is, the viruses were attenuated (26). In one macaque infected with SIVmac239-Y/I, however, the codon for I reverted to a codon encoding Y within 12 weeks after infection. The clinical course of this animal paralleled those of animals inoculated with wild-type SIVmac239.

During the initial 12 months of a second study designed to determine whether attenuation resulted from differential interactions with the immune system, it appeared that $CD16^+$ NK cells gradually were being depleted in those animals with the highest virus burdens and SIV-specific antibody titers. However, the putative loss of NK cells was observed only when cells in EDTA-treated whole blood, not cells in purified peripheral blood mononuclear cells (PBMC), were evaluated by flow cytometry. The results of experiments to explain this phenomenon, using blood samples from a subset of macaques from a larger study, are reported here. Details of the comprehensive study to evaluate changes in multiple virological, hematological, and SIVmac239-specific immunological parameters associated with these and additional animals infected with other SIVmac239 variants will be published elsewhere.

MATERIALS AND METHODS

Animals and virus inoculations. Six juvenile female pig-tailed macaques (*Macaca nemestrina*), seronegative for antibodies to SIV, simian T-cell leukemia virus, simian type D retroviruses, and herpesvirus type B, were used in this study. Limited results from two additional animals (98P016 and 99P032) are presented for comparison and as control responses. All animals were housed in isolation facilities at the University of Alabama at Birmingham (UAB) and cared for in accordance with institutional and Animal Welfare Act guidelines. The protocol was approved by the UAB Institutional Animal Care and Use Committee. The macaques were randomly placed in two groups and inoculated intravenously with 10^3 50% tissue culture infective doses of either wild-type SIVmac239 or SIVmac239-Y/I, in which the tyrosine at amino acid 721 in the cytoplasmic tail was mutated to isoleucine (42). After virus inoculation, blood samples were collected from each animal at regular intervals to monitor changes in lymphocyte populations, including $CD16^+$ $CD3^-$ and $CD16^+$ $CD3^+$ cells, which define macaque NK and putative NKT cells, respectively.

Immunofluorescence flow cytometry. Percentages of $CD16^+$ cells were determined by two-color flow cytometry with mouse anti-human MAbs labeled with different fluorochromes—phycoerythrin (PE)-conjugated CD16 (clone 3G8) and fluorescein isothiocyanate (FITC)-conjugated CD3ε (clone SP34)—that are known to be cross-reactive with macaque antigens. For the whole-blood analysis, 50 μl of EDTA-treated blood was used, and in some cases the volume was increased to 100 μl because of lymphopenia late in infection. Aliquots of blood were incubated with 10 μl of each of the two MAbs or with isotype controls for 30 min at room temperature. Contaminating erythrocytes were lysed with fluorescence-activated cell sorter (FACS) lysing buffer, followed by one wash with cold phosphate-buffered saline (PBS) containing 0.1% sodium azide. Two other PE-conjugated MAbs, CD8α (clone SK1) and CD7 (clone M-T701), were used in combination with CD3ε-FITC to confirm the identity of NK populations in blood. PBMC were isolated from heparinized whole blood by centrifugation through lymphocyte separation medium (ICN Biomedicals Inc., Aurora, OH); aliquots of fresh PBMC (4×10^5 cells) were mixed with 10 μl of each MAb and processed as described for whole blood, omitting incubation with lysing buffer. Cell-associated immunofluorescence was analyzed within 1 day on a FACSSTAR flow cytometer. Lymphocytes were gated according to forward-scatter versus side-scatter characteristics; negative cell populations, identified with isotype-matched control antibodies, were excluded. All antibodies, reagents, and the flow cytometer were purchased from BD Biosciences Pharmingen (San Diego, CA).

Enrichment of NK cell populations and immunoblotting. To detect CD16 protein expressed in cells, NK populations were enriched from PBMC. Briefly, $CD16^+$ monocytes were removed by culturing PBMC overnight in RPMI 1640 medium with 15% fetal bovine serum in T75 plastic tissue culture flasks. Nonadherent cells were collected and washed twice with PBS containing 2% fetal bovine serum. Cells were then incubated with Dynabeads prepared by coupling a mouse anti-monkey CD3 MAb (clone FN18; 1 μg/μl; Biosource, Camarillo, CA) to mouse pan-IgG Dynabeads (Dynal Biotech Inc., Norway) for 30 min at room temperature to remove $CD3^+$ T cells. The remaining cells, which included NK and B cells, were lysed with M-PER (mammalian protein extraction reagent; Pierce, Rockford, IL) supplemented with 1 mM phenylmethylsulfonyl fluoride, 1 mM sodium orthovanadate, and 0.1% aprotinin. Supernatants were collected by centrifugation; equal amounts of protein (50 μg/well), quantified by a Bio-Rad Dc protein assay (Bio-Rad Laboratories, Hercules, CA), were separated by sodium dodecyl sulfate-polyacrylamide gel electrophoresis on 10% gels. Proteins were transferred electrophoretically to nitrocellulose membranes (Schleicher & Schuell Bioscience, Inc., Germany) and immunoblotted with anti-CD16 MAbs or antibodies to an internal control, β-actin (clone AC-15; Sigma, St. Louis, MO). Antibodies bound to the CD16 or β-actin proteins were detected by incubation with horseradish peroxidase-conjugated secondary antibodies (Santa Cruz Biotechnology, Santa Cruz, CA), developed using a SuperSignal West Pico kit (Pierce), and quantified by using an AlphaImager system and AlphaEase software (Alpha Innotech Corp., San Leandro, CA). A prestained protein ladder (Invitrogen Corp., Carlsbad, CA) was used as a molecular size standard.

Purification of total IgG. Total IgG was purified from plasma samples by using a HiTrap Protein G Hp column (MABTrap kit; Amersham Biosciences, Piscataway, NJ) according to the manufacturer's suggested protocol. Briefly, plasma samples were filtered through a 0.45-μm-pore-size filter, mixed with binding buffer (20 mM sodium phosphate, pH 7.0) at a 1:1 ratio, and applied to the column. The column was washed with approximately 7 ml of binding buffer, and 1-ml fractions were collected. Total IgG was then eluted from the column with approximately 5 ml of elution buffer (0.1 M glycine-HCl, pH 2.7). Immediately after elution, each 1-ml fraction of total IgG was neutralized with 75 μl of 1 M Tris-HCl, pH 9.0. The absorbance of total IgG (optical density at 280 nm) was measured with a DU 640 spectrophotometer (Beckman, Fullerton, CA) and multiplied by a conversion factor of 0.75 to determine IgG concentrations.

Blocking of CD16 (FcγRIIIa) with plasma and serum samples and purified IgG. To assess the abilities of blood components and total IgG to inhibit binding of MAb 3G8 to CD16, 1×10^6 PBMC were incubated with varying amounts of plasma, serum, or purified IgG for 30 to 45 min at 37°C. Mixtures were aliquoted; 3.3×10^5 cells were incubated with excess amounts of CD16-PE and CD3ε-FITC or control antibodies, washed twice with cold PBS containing 0.1% sodium azide, and analyzed for immunofluorescence as described above.

Quantification of viral RNA, SIV antibodies, and p27 antigen. SIV RNA plasma viremia (sensitivity, less than 100 copies/ml) was quantified at the Quantitative Molecular Diagnostics Core of the AIDS Vaccine Program, SAIC Frederick, NCI (Frederick, MD), as described previously (46). SIV-specific antibody titers in serum samples were determined after twofold serial dilutions using a

highly cross-reactive HIV type 2 enzyme immunoassay kit (Bio-Rad). Both flowthrough and eluted fractions from protein G columns were assayed for SIV $p27^{gag}$ antigen with a commercial enzyme immunoassay kit (Zeptometrix Corp., Buffalo, NY). The specimens were treated with PBS containing 10% Triton X-100 (pH 7.2) before addition to the test plate. Free SIV $p27^{gag}$, $p27^{gag}$ released from intact virions, and $p27^{gag}$ released from ICs that contained IgG and either $p27^{gag}$ or SIV virions were detected with this assay.

Measurement of NK cell activity. NK cytolytic activity against the NK-sensitive human erythroleukemic cell line K562 was measured using a two-color flow cytometric assay that utilized two fluorescent dyes (12, 38): DIO (D275; Molecular Probes, Inc., Eugene, OR), a lipophilic carbocyanine membrane dye, was used to label live K562 target cells, and propidium iodide (PI; Sigma) was used to stain nuclear DNA in the prelabeled K562 cells after membrane permeabilization. K562 target cells maintained in 10% RPMI 1640 (10%-RPMI) were seeded daily for 3 days at a concentration of 2×10^5 cells/ml, after which 3×10^6 target cells were incubated in 10 μl of 3 mM DIO for 20 min at 37°C, washed with PBS, and resuspended in 10%-RPMI at a concentration of 1×10^6 cells/ml. Effector NK cells ($CD16^+$ $CD3^-$), enriched as described above, were washed twice with 10%-RPMI, and appropriate numbers were then transferred to each of five assay tubes to yield final effector-to-target (E:T) cell ratios of 20:1, 10:1, 5:1, and 2.5:1; a tube with effector cells only was used as a negative control. After the volumes were adjusted to 130 μl by pelleting cells and either removing excess or adding additional medium, as required, 2×10^4 DIO-stained target cells (in 20 μl) were added to each of these tubes and to control tubes containing either target cells only or target cells with 10 μl of 1% Triton X-100, as spontaneous or maximum lysis controls, respectively. To each tube 130 μl of PI working solution (0.1 mg/ml in 10%-RPMI) was added, followed by a brief centrifugation, to optimize effector-target cell contact, and incubation at 37°C for 2 h; then the cells were resuspended and analyzed by FACS. When the effect of IgG/IgG-ICs on NK cell activity was tested, the enriched effector cell population was incubated with total IgG in a volume of 1 ml for 45 min and then added directly to assay tubes, without washing, to yield the different E:T ratios. Alternatively, the enriched NK cells were aliquoted to individual tubes to establish the different E:T ratios, and then appropriate amounts of purified IgG were added to each tube to maintain a constant ratio of 1 mg IgG/1×10^6 cells. After the volume was adjusted to 130 μl, the mixture was incubated 45 min before addition of the K562 target cells. The target cells only, target cells with Triton X-100, and effector cell controls were used to set the gates in DIO-versus-PI dot plots. Viable DIO-stained or damaged target cells were identified by green fluorescence or both green and red fluorescence, respectively. Percent lysis, expressed as the percentage of cells that were DIO^+ PI^+, was calculated as (number of DIO^+ PI^+ cells)/(number of DIO^+ PI^+ cells + number of DIO^+ PI^- cells) × 100. Percent specific lysis was determined by subtracting the percent spontaneous lysis of the target cells only from the percent lysis at each E:T ratio. To calculate lytic units (LU), a simplified computational method, utilizing formula 12 as described by Bryant et al. (8), was used. First, the number of cells in 1×10^7 effector cells that was required to lyse 10% of the target cells ($LU_{10}/10^7$ effector cells) was calculated. Then this value was converted to the number of $LU_{10}/10^6$ NK cells that were present in the enriched effector cell population.

RESULTS

Apparent loss of $CD16^+$ cells after SIV infection. Six macaques were inoculated intravenously with virus stocks generated from transfection of CEMx174 cells with one of two molecularly cloned viruses; three animals (99P040, 99P041, 99P051) received SIVmac239, and the other three (98P029, 98P062, 99P006) received the SIVmac239-Y/I mutant. After virus inoculation, the percentages of lymphocyte subsets, including $CD16^+$ $CD3^-$ or $CD16^+$ $CD3^+$ cells, in whole blood were monitored. During the first 10 weeks of infection, the three SIVmac239-infected animals exhibited frequent fluctuations in total percentages of both $CD3^+$ and $CD3^-$ $CD16^+$ cells (Fig. 1A). After 10 weeks of infection, percentages of total $CD16^+$ cells in blood from macaque 99P040 decreased rapidly and essentially became undetectable (<1%) at 22 weeks, while the percentages of $CD16^+$ cells in macaques 99P051 and 99P041 progressively declined and were undetectable (<1%) at 39 and 68 weeks, respectively. In animals exposed to the SIVmac239-Y/I mutant, after 10 weeks of infection, the changes in percentages of $CD16^+$ cells in 99P006 and 98P062 were similar to those in 99P040 and 99P051 (Fig. 1B). In contrast, the percentage of $CD16^+$ cells in whole blood from 98P029 remained relatively high for about 85 weeks, after which time the population of $CD16^+$ cells quickly fell to undetectable levels during the following 9 weeks. Associated with the observed decline or loss in percentages of $CD16^+$ cells in whole blood, the mean fluorescence intensity (MFI) of CD16 on cells in whole blood gradually decreased after infection until it appeared that all circulating $CD16^+$ cells eventually were lost (Fig. 2). The actual time course over which the decrease in MFI of antibodies bound to CD16 was observed differed among the animals, but the general pattern was identical for all six animals. Analyses of putative absolute numbers of $CD16^+$ cells, which are calculated from the percentages determined by FACScan, mirrored the results presented here.

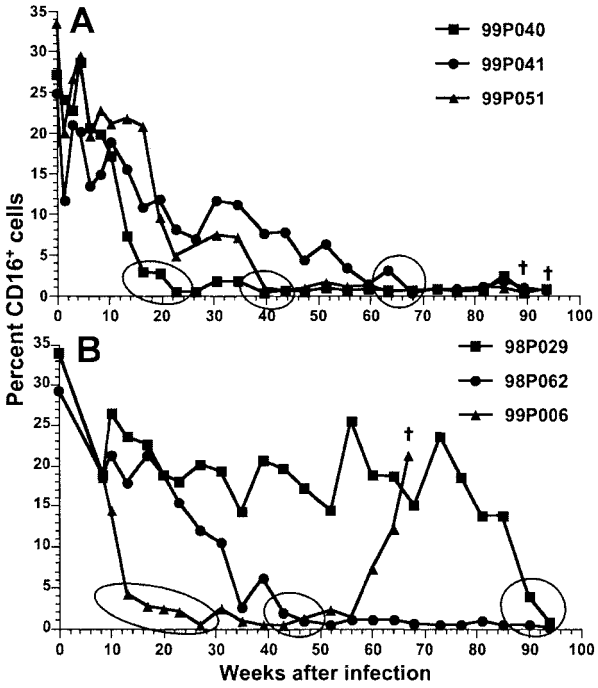

FIG. 1. Changes in percentages of $CD16^+$ cells in whole blood from macaques inoculated with SIVmac239 (A) or SIVmac239-Y/I (B). Circles or ovals indicate the intervals during which the CD16 MFI reached levels consistent with those of $CD16^-$ cell populations. †, euthanasia as a result of SIV-induced disease.

Our previous study showed that in SIVmac239-Y/I-infected animals the mutation to isoleucine at position 721 reverted to a tyrosine in some PCR clones obtained from PBMC at 12 weeks after infection (26). When the Y-dependent motif in viruses from the three SIVmac239-Y/I-infected animals was sequenced at 13 weeks after infection, all clones generated from both 98P062 and 99P006 had reverted to tyrosine. Among eight clones from 98P029 that were analyzed, an isoleucine at position 721 was present in two while a tyrosine was present in six clones. These data showed that reversion of I to Y at amino acid 721 occurred early after infection and was associated with the apparent early loss of cells expressing CD16 and a progressive decrease in MFI for CD16. The fact that 98P029 main-

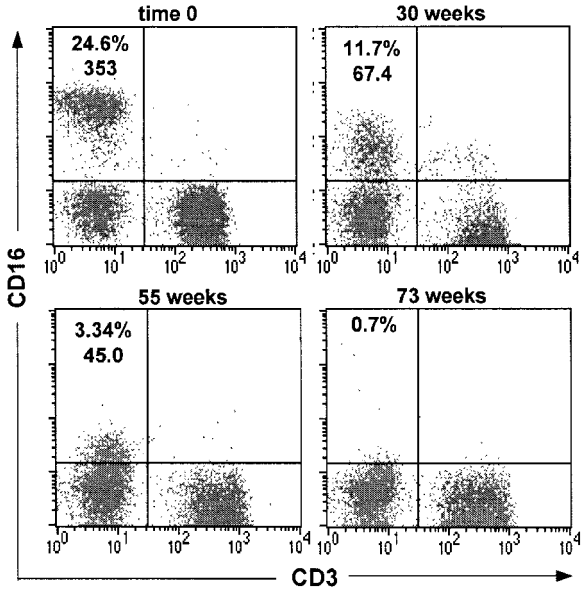

FIG. 2. Analysis of $CD16^+$ cells in the lymphocyte gates of whole blood collected from macaque 99P041. The results are representative of those obtained from analyses of blood from all six animals. The times after infection when each FACScan profile was obtained are shown above each panel. The numbers in the upper left quadrants are percentages of $CD16^+$ $CD3^-$ NK cells and the MFI for CD16 staining in each quadrant. For FACScan profiles shown in all figures, MFIs are not provided if the number of events in a quadrant were too few and scattered, leading to aberrant MFIs.

tained detectable $CD16^+$ cells in blood might have been related to the finding that, of the six animals, this one had the lowest level of SIV RNA in plasma during the first few weeks after infection (data not shown). However, between 65 and 78 weeks, the amount of plasma virion RNA in this animal increased to the level ($>1 \times 10^5$ copies/ml) detected in the other animals and was accompanied by putative decreases in the number of $CD16^+$ cells. The kinetics of anti-SIV antibody titers and their maximums were the same for all six animals, except that the highest titers for macaque 98P029 were achieved gradually, in parallel with increases in virion RNA levels in plasma.

The one anomaly in the apparent gradual loss of $CD16^+$ cells in blood occurred with macaque 99P006. After a rapid decrease and maintenance of low numbers of $CD16^+$ cells for approximately 40 weeks, the percentages of these cells detected in whole blood began to increase at 60 weeks after infection, and this trend continued until the death of the animal at 67 weeks (Fig. 1B). The reason for this reversal is not known, since both levels of cell-free virion RNA in plasma and antibody titers remained high. It is possible, however, that CD16 acquired a mutation in one of its extracellular domains that impaired ligand binding such that ICs no longer blocked binding of MAb 3G8 to CD16 (see below). Mutations that inhibit binding of mIgG and ICs to CD16 have been described and predispose humans to autoimmune diseases (69).

Detection of NK cells in blood. Because it was possible that $CD16^+$ $CD3^-$ NK cells were still present in blood and that the failure of MAb 3G8 to recognize CD16 on cells was an artifact, two other surface markers associated with both human and macaque NK and T cells, CD8α and CD7, were evaluated (9, 58). A previous study, which is supported by our unpublished results, demonstrated that in macaques a majority of $CD16^+$ lymphocytes coexpress CD8α and that CD7 is expressed on about 90% of rhesus $CD16^+$ $CD8\alpha^+$ double-positive NK cells (9, 68). By using a MAb to CD3ε in combination with either a MAb to CD7 or a MAb to CD8α, NK cell populations can be distinguished from $CD3^+$ T and NKT cells. $CD7^+$ $CD3^-$ and $CD8\alpha^+$ $CD3^-$ populations were detected in whole blood from all animals in which few or no (<1%) $CD16^+$ cells were apparent. As an example, although less than 1% of cells in whole blood from 99P006 at 35 weeks after virus inoculation were $CD16^+$, 14.3 and 11.1% of the cells were $CD8^+$ $CD3^-$ and $CD7^+$ $CD3^-$, respectively (Fig. 3). These results indicated that the gradual decrease in the number of $CD16^+$ cells and the eventual inability to detect $CD16^+$ cells in whole blood were not real and probably did not represent an actual loss of NK cell populations.

In an attempt to isolate the $CD7^+$ $CD3^-$ or $CD8\alpha^+$ $CD3^-$ cells, PBMC were obtained and depleted of adherent and $CD3^+$ cells; the remaining cells were analyzed by flow cytometry to confirm depletion of T cells. Unexpectedly, expression of CD16 with high MFI was detected on enriched $CD3^-$ NK cells. CD16 is a low-affinity receptor for the Fc region of IgG, and MAb 3G8 binds at or near the CD16 ligand-binding site and competes for binding with the Fc portion of IgG (22, 63). Binding of MAb 3G8 to CD16 would be inhibited when all CD16 molecules were saturated with IgG-ICs at physiological

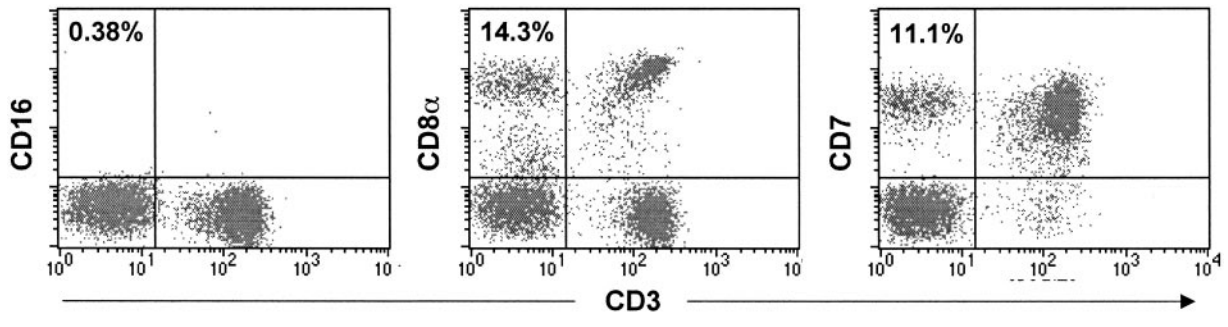

FIG. 3. Detection of $CD16^+$ $CD3^-$, $CD8\alpha^+$ $CD3^-$, and $CD7^+$ $CD3^-$ cell populations in whole blood collected from macaque 99P006 (35 weeks). The putative percentages of NK cells with the indicated immunophenotypes are shown in the upper left quadrant of each FACScan plot. The $CD3^+$ populations in the upper and lower right quadrants are T cells.

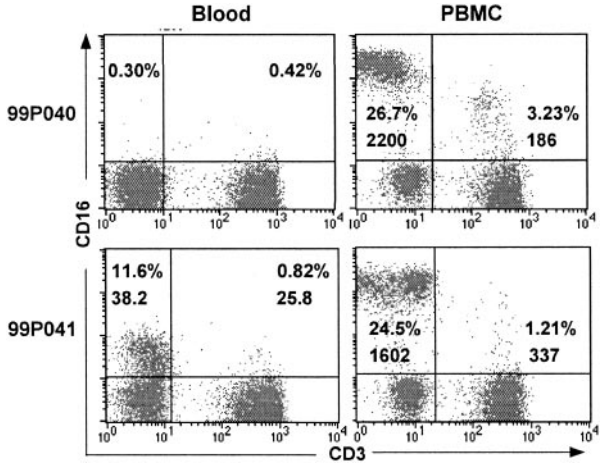

FIG. 4. Comparison of CD16$^+$ cell populations detected in whole blood and PBMC obtained from macaques 99P040 and 99P041 at 35 weeks after infection. Numbers in upper left and right quadrants indicate CD16 percentages and MFIs for cells in the two quadrants.

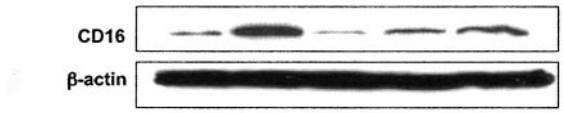

Lane	1	2	3	4	5
Animal	P062	P032 [a]	P040	P041	P051
Weeks p.i.	35	27	27	27	27
# CD16$^+$ cells/μl [b]	102	973	18	219	13
% CD16$^+$ cells [c]	19.6	83.9	60.9	38.1	67.7
CD16:β-actin	0.12	0.64	0.04	0.21	0.38
Normalized ratio	0.61	0.76	0.07	0.55	0.56

[a] Negative control animal with no decrease in the percentage or MFI of CD16.

[b] Putative absolute number of CD16$^+$ cells in whole blood at the indicated times after infection.

[c] Percentage of CD16$^+$ cells after enrichment of PBMC by negative selection.

FIG. 5. Expression of CD16 in NK cells enriched from PBMC of macaques with different percentages of CD16$^+$ cells detectable in whole blood. The ratio of CD16 to β-actin was determined using areas under the curves of the respective bands, measured with an AlphaImager. The relative intensity or normalized ratio (CD16:β-actin ratio) for each animal was determined by dividing each ratio by the percentage of CD16$^+$ cells in the enriched PBMC fractions and multiplying by 100.

concentrations, but during isolation of PBMC, the ligands would dissociate from CD16, making it available to MAb 3G8. To test this hypothesis, flow cytometry was performed with whole blood and PBMC isolated from the same blood samples of all six animals. As expected, the MFIs of CD16 and the percentages of CD16$^+$ cells in PBMC were substantially higher than those in whole blood (Fig. 4). For the representative dot plots shown in Fig. 4, the changes in percentages of total CD16$^+$ cells (percentages in upper left plus upper right quadrants) increased from <1% in blood to approximately 30% in PBMC from macaque 99P040 and from 12.4 to 25.7% in PBMC from 99P041. In addition, the MFI for CD16 expression in CD3$^-$ cells from the latter animal increased more than 40-fold (from 38.2 to 1,602) after separation of PBMC from whole blood and removal of plasma.

Detection of CD16 protein in cell lysates. It was possible that some of the observed differences in CD16 expression on cells between whole blood and PBMC were associated with down-regulation of CD16 protein expression in NK cells. To test this possibility, immunoblot analyses of lysates of enriched NK cells were performed using the anti-CD16 MAb 3G8. Lysates of cells from the three SIVmac239-infected animals (99P040, 99P041, 99P051) at 27 weeks, from one SIVmac239-Y/I-infected animal (98P062) at 35 weeks, and, as a control, from one animal (99P032) infected with a related attenuated SIVmac239 variant that had no apparent loss of CD16$^+$ cells were tested. The apparent percentages and absolute numbers of CD16$^+$ cells in whole-blood samples from these animals ranged from 0.45 to 29.3% (not shown) and from 13 to 973 cells/μl, respectively (Fig. 5, number of CD16$^+$ cells/μl). CD16 protein was found in cell lysates from all animals. To compare CD16 expression levels among these five animals, the intensities of CD16 protein bands relative to those of an internal control protein, β-actin, in each lysate were calculated and normalized to 100% NK cells, which was necessary because of differences in the extent of enrichment (Fig. 5, percent CD16$^+$ cells) of the NK cells from different animals. The levels of CD16 expression (Fig. 5, normalized ratio), designated by relative intensities [(CD16/β-actin ratio)/(percent CD16$^+$ cells) × 100], were similar for 98P062, 99P041, and 99P051 despite differences in putative percentages and numbers of CD16$^+$ cells in whole blood. Of note, although the percentage of CD16$^+$ cells in whole blood from the control animal (99P032) was markedly higher (29.3%), no significant differences in CD16 expression levels were observed between three of the four infected macaques and the control animal. The exception was macaque 99P040, which appeared to have 10-fold-lower expression of CD16. It is possible that this finding was related to the fact that this animal had had blocked recognition of CD16 in whole blood longer than any of the other animals, resulting in down-regulation of expression of CD16.

Inhibition of CD16-3G8 interactions by macaque plasma. To investigate whether recognition of CD16 molecules on NK and CD16$^+$ CD3$^-$ NKT cells in blood of infected animals was blocked by IgG or ICs and whether the failure of MAb 3G8 to bind CD16 was dependent on the amount of available ligands, dose-response experiments were performed with plasma samples obtained from macaque 99P006 on day 0 (PL006/0) and at 39 weeks (PL006/39) after infection; CD16$^+$ cells had not been detected in whole blood in this animal since week 27. In addition, plasma obtained at 47 weeks (PL016/47) from an animal (98P016) with nonprogressive SIVmac239 infection that had exhibited no decrease in CD16 MFI (data not shown) was used as a negative-control sample. (Macaque 98P016 had rapidly controlled and maintained virion RNA levels in blood at <100 copies/ml since 10 weeks after inoculation, and its antibody titers to SIVmac239 had fluctuated between 6,400 and 12,800 for more than 90 weeks.) Freshly isolated macaque PBMC were incubated with varying amounts of plasma samples—

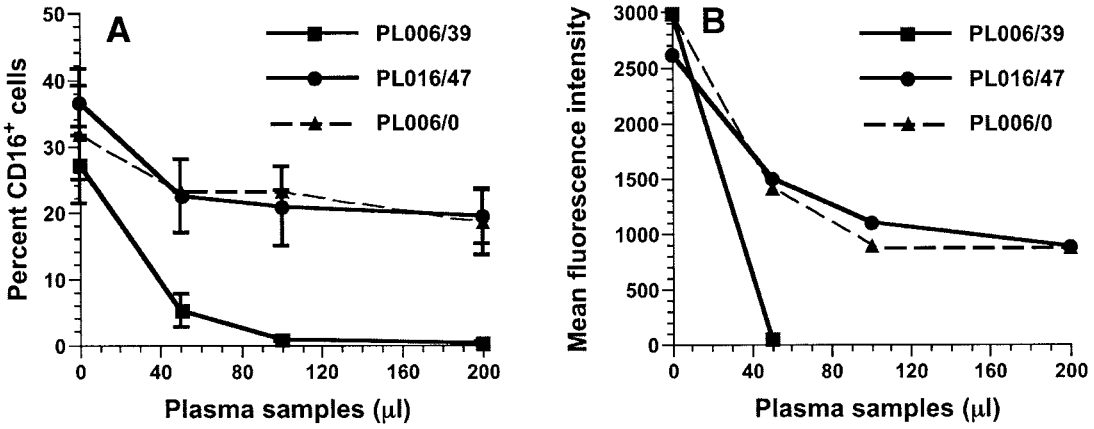

FIG. 6. Plasma inhibition of recognition and binding of MAb 3G8 to CD16. PBMC from macaques were incubated with increasing amounts of plasma from macaque 99P006 or 98P016, and the residual percentages of $CD16^+$ cells (A) and the respective MFIs of CD16 (B) were evaluated. The data points represent mean values for plasma samples from each animal; plasma collected from 99P006 and 98P016 at 39 and 47 weeks after infection, respectively, was tested with PBMC from three different macaques. Plasma samples collected from 99P006 before infection were tested on two occasions with PBMC from three different macaques ($n = 6$).

PL006/0, PL006/39, or control PL016/47—before addition of MAb 3G8-PE. As the volume of PL006/39 increased from 0 to 200 μl (in 50-μl increments), a decline in the apparent percentage of $CD16^+$ cells was observed (Fig. 6A): inhibition of MAb 3G8 binding to CD16 with 50, 100, and 200 μl of PL006/39 from macaque 99P006 was 81, 97, and 99%, respectively. In contrast, the observed percent decrease of $CD16^+$ cells in the presence of 50 μl of PL006/0 from macaque 99P006 was 28%, with a maximum of 38% when 200 μl of PL006/0 was added. Incubation of cells with the same volumes of the control plasma from the infected nonprogressor macaque (98P016) gave equivalent reductions in MAb 3G8 binding. Moreover, the maximal effect on the MFI of CD16 was achieved with 100 μl of PL006/0: the MFI of the CD16-3G8 interaction decreased 3.3-fold (Fig. 6B). Similar results were obtained when cells were incubated with serum (instead of plasma) obtained on day 0 and at 43 and 47 weeks from 99P006 (data not shown). The data obtained using 99P006's day-0 plasma or serum samples also indicated that percentages and numbers of $CD16^+$ cells in whole blood were, in general, underestimated by MAb 3G8, because recognition of and binding to CD16 were partially blocked under normal physiological conditions due to CD16 recognition and binding of the fluctuating amounts of mIgG and/or IgG-ICs that always circulate in normal blood.

Correlation between numbers of $CD16^+$ cells, SIV antibody titers, and viral loads. All six animals had not only high serum antibody titers to SIVmac239 (range, 51,200 to 1,638,400 [4.71 to 6.21 $\log_{10}$]) but also high virion RNA copy numbers (4.79 to 6.32 $\log_{10}$ copies/ml) in plasma during the time the decline in the MFI of MAb 3G8 binding to CD16 was observed; therefore, it was likely that IgG-associated ICs, especially SIV-containing ICs, played a major role in blocking interactions between CD16 and MAb 3G8. When the relationships between the apparent absolute numbers of $CD16^+$ cells detected in whole blood and serum antibody titers or plasma viral loads were analyzed (Spearman correlation), the apparent absolute number of $CD16^+$ cells correlated inversely with both SIVmac239 antibody titers and viral loads (Fig. 7). Collectively, these results supported the idea that SIV-ICs gradually increased as the concentration of antibodies to SIVmac239 increased, ultimately reaching a level at which the binding of MAb 3G8 to CD16 on NK and NKT cells was inhibited completely. In animals such as 98P016 with low viral burdens and low antibody titers, and thus fewer circulating ICs, saturation of CD16 probably did not occur and some CD16 was available for subsequent MAb 3G8 binding in the FACS analysis.

Blocking of CD16-3G8 interaction by SIV-ICs. Levels of HIV-ICs and ICs containing antigens from concurrent micro-

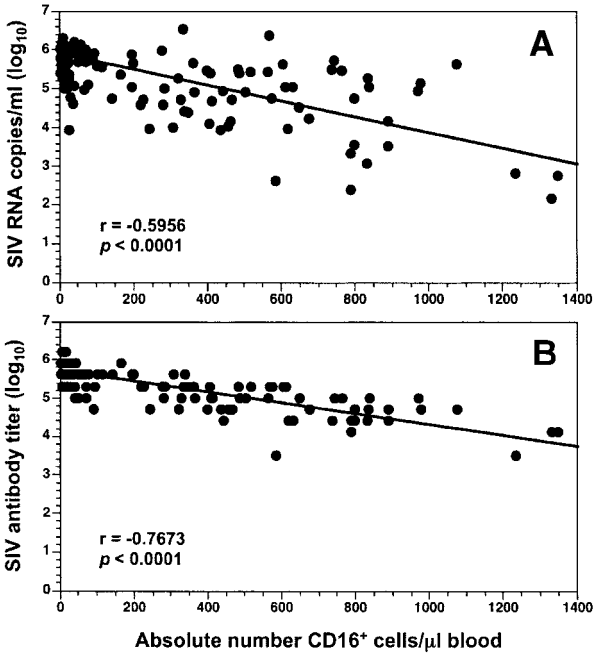

FIG. 7. Correlation between apparent absolute numbers of $CD16^+$ cells in whole blood and either plasma viral RNA levels (A) or SIV antibody titers (B). Data obtained between 4 and 94 weeks for the three SIVmac239-infected animals and between 8 and 94 weeks (inclusive) for the three SIVmac239-Y/I-infected animals were combined for both analyses (Spearman correlation).

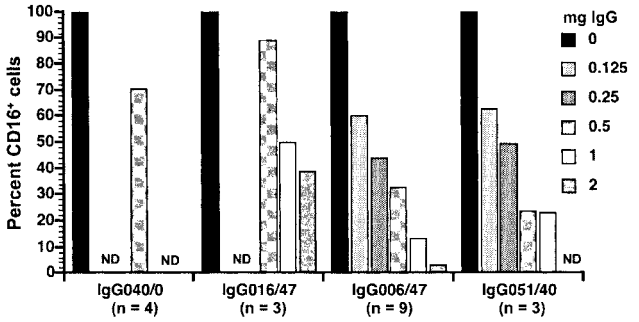

FIG. 8. Inhibition of binding of MAb 3G8 to CD16 on the cell surface by purified IgG and IgG-ICs. Values shown are percentages of the value for the control (100%) to which no IgG was added. Total IgG and IgG-ICs were purified from plasma samples either from progressors (99P006 and 99P051), from a nonprogressor (98P016), or from 99P040 before infection (IgG040/0). These IgG preparations, designated by the last three digits of the animal identification number and the number of weeks after infection (e.g., IgG006/47), were tested by using PBMC from uninfected macaques and evaluating the percentages of $CD16^+$ cells after incubation with different amounts of the purified IgG/IgG-ICs. The numbers of independent experiments performed using the various IgG/IgG-ICs are given below the plasma designations; the value for the percentage of $CD16^+$ cells is the mean of values from all experiments with a particular IgG/IgG-IC preparation. For some IgG preparations, not all concentrations were tested the same number of times. Omission of a bar at a particular IgG concentration indicates that the concentration was not tested (not determined [ND]).

bial infections are elevated in HIV-infected patients (52); relative to healthy controls, significant differences in the levels of both types of ICs are observed. Because animals in our study were housed in an isolation facility, the chance for them to acquire secondary infections was probably lower than that for HIV-infected humans. Thus, it is probable that most IgG-ICs circulating during chronic progressive SIVmac239 disease, which is associated with high viral loads and antibody titers, are SIV-ICs. If this conclusion is valid, total IgG purified from plasma samples from 98P016, with nonprogressive SIV infection, undetectable virus, and low antibody titers, would contain relatively lower concentrations of SIV-ICs. In contrast, total IgG isolated from plasma samples obtained from animals with no detectable $CD16^+$ cells would consist primarily of SIV-ICs. To test this assumption, total IgG was purified by passage of plasma samples over protein G-Sepharose columns. The plasma components not bound to protein G migrated through the column in the wash buffer (flowthrough fraction); those eluted from the protein G column contained total IgG, including IgG-ICs. IgG was purified using plasma samples from 99P006 at 47 weeks, from 99P051 at 40 weeks, from 98P016 at 47 weeks, and from 99P040 before infection (day 0). In order to have enough purified IgG from macaque 99P006 for several experiments, total IgG in four 1-ml aliquots of plasma from this animal was isolated independently; eluted fractions with the highest optical densities at 280 nm were used. When 100- and 200-μl aliquots of all flowthrough fractions were incubated with 1×10^6 PBMC, followed by addition of an excess amount of MAb 3G8 (10 μl/3.3×10^5 cells), the percentages of $CD16^+$ cells and the MFIs of CD16 were not different from those obtained without the addition of each plasma fraction (not shown). These results demonstrated that components in the flowthrough had no effect on blocking MAb 3G8 binding to CD16 even though soluble $p27^{gag}$ antigen was present in these fractions (range of $p27^{gag}$ protein concentrations, 8 to 60 pg/ml).

Using PBMC from different macaques, the apparent percentages of $CD16^+$ cells progressively decreased as the amount of purified IgG (containing SIV-ICs and unrelated ICs) from macaques 99P006 and 99P051 was increased from 0 to 2 mg in twofold increments; a maximum of 97% inhibition was observed in the presence of 2 mg of total IgG from 99P006 (Fig. 8). The $p27^{gag}$ antigen concentration in the purified IgG pools from macaques 99P006 and 99P051 ranged from 8 to 48 pg/ml, confirming that total IgG from both macaques contained SIV-ICs. Although the degree of inhibition of MAb binding to CD16 differed among animals and in independent experiments, the mean percent inhibition that occurred with different amounts of IgG clearly showed a dose-dependent decrease in the ostensible percentages of $CD16^+$ cells in PBMC. Comparison of the percent inhibition of MAb 3G8 binding to CD16 observed with 0.5 mg of IgG from the two progressors with the percent inhibition observed with the same amount of IgG from the nonprogressor (98P016) and preinfection plasma donor (99P040) macaques revealed distinct differences in the abilities of IgG/IgG-ICs from the latter two animals to inhibit binding. In fact, 1 to 2 mg of IgG from 98P016 was required to obtain the same degree of inhibition as 0.125 and 0.25 mg of IgG/IgG-ICs from 99P006 and 99P051. This difference indicated that about eightfold more IgG/IgG-ICs were required to block MAb 3G8 binding, which most likely can be explained by the disparate plasma virion RNA levels and serum SIV-specific antibody titers in the three infected animals (Table 1). The inhibition observed with IgG/IgG-ICs isolated from the nonprogressor and uninfected animals can be attributed to much smaller amounts of IgG and IgG-ICs formed with SIV and antigens unrelated to SIV. Taken together, these data demonstrate that recognition of CD16 expressed on NK (and NKT) cells in chronically infected animals with high viral loads and titers of SIV-specific antibodies was blocked primarily by SIV-ICs and that the extent of inhibition of MAb 3G8 binding to CD16 was related to the amount of SIV-ICs present in whole blood, plasma, and the purified IgG fractions.

Effect of IgG/IgG-ICs on NK cell activity. To determine whether the presence of IgG/IgG-ICs in blood might affect NK cell activity, $CD16^+$ $CD3^-$ cells were enriched from PBMC from two healthy and two SIVmac239-infected animals. Com-

TABLE 1. Differences in apparent numbers of $CD16^+$ NK cells in whole blood and purified PBMC from SIV-infected macaques at the time when IgG was purified from plasma

Macaque	Viral RNA[a] concn (copies/ml)	Antibody titer	$p27^{gag}$ concn[b] (pg/ml)	% (no.) of $CD16^+$ cells[c] in:	
				Whole blood	PBMC
98P016	<100	12,800	0	13.4 (245)	18.4 (337)
99P006	390,000	819,200	48	0.78 (4)	27.2 (151)
99P051	111,000	1,638,400	15	0.89 (18)	49.1 (1,018)

[a] SIVmac239 virion RNA in plasma at the time when IgG was purified.
[b] Amount of SIV $p27^{gag}$ in the IgG fractions after purification on protein G-Sepharose columns.
[c] Obtained by FACScan using a whole-blood assay or purified PBMC and from complete blood counts and differentials, respectively.

TABLE 2. Effect of IgG/IgG-IC blocking of the MAb 3G8–CD16 interaction on NK cell activity against K562 cells

IgG source[a]	Inhibition of 3G8 binding (%)[b]	Median $LU_{10}/10^6$ NK cells[c]	% of control[d]	No. of assays[e]
None		6.68	100	7
IgG006/0, IgG016/0	34	5.72	96	4
IgG016/47	15	4.67	97	4
IgG006/47 or IgG006/52	96	8.15	117	5

[a] Assays were done using 1 mg of each IgG/IgG-IC preparation and enriched NK cells.

[b] In each experiment, percent inhibition was calculated from the percentage of $CD16^+$ $CD3^-$ cells that were detected by FACScan after incubation of 1 mg of purified total IgG with an enriched NK cell population. Values shown represent mean percent inhibition relative to the percentages of $CD16^+$ $CD3^-$ cells in the enriched populations.

[c] There was no significant difference in $LU_{10}/10^6$ NK cells when means for the various sources of purified IgG were compared with that for the control (Student's *t* test).

[d] The 100% control represents the mean $LU_{10}/10^6$ NK cells in individual assays for each enriched NK cell population that was not incubated with purified IgG before addition of K562 target cells.

[e] Results obtained using effector cells from both uninfected and SIVmac239-infected macaques were combined to determine means for percent inhibition and median LUs.

pared to those in PBMC, the percentages (range, 41.5 to 78%; average, 55.1% [for eight experiments]) as well as numbers of NK cells in the populations used as effector cells were higher in these enriched populations. Therefore, we reassessed whether total IgG from 98P016 (at day 0 and at 47 weeks) and 99P006 (at day 0 and at 47 and 52 weeks) would block the presumed larger number of CD16-3G8 interactions. (Additional IgG pools were purified from 99P006's plasma obtained at 52 weeks after infection; the SIV $p27^{gag}$ antigen concentration ranged from 7.7 to 21 pg/ml.) Blocking assays using 1×10^6 enriched cells and 1 mg of purified IgG from day-0 plasma from 98P016 and 99P006, 47-week plasma from 98P016, and 47- and 52-week plasma from 99P006 showed that the interactions between CD16 and 3G8 were blocked only when purified IgG/IgG-ICs obtained from 99P006 at late times after infection were added (Table 2). Inhibition of CD16-3G8 binding by total IgG purified from the day-0 plasma and the IgG016/47 sample was similar to that obtained when eightfold less (0.125 mg; 25% inhibition) IgG/IgG-ICs from 99P006 were used. These results are comparable to those obtained when PBMC were used to demonstrate blocking of CD16-3G8 binding by IgG/IgG-ICs (Fig. 8) and indicated that 1 mg of purified IgG was sufficient for use in lytic assays with enriched NK cells.

Regardless of whether blocking IgG/IgG-ICs were present, that is, whether the IgG was obtained from 99P006 after infection, incubation of NK cell-enriched populations with various purified IgG preparations before testing for lytic activity against K562 cells had no inhibitory effect on cell killing (Table 2). In fact, in individual assays, compared to the control to which no IgG was added, there was a trend toward augmentation of the calculated number of LUs when purified IgG was present. Even when the assay protocol was varied by adding purified IgG from 99P006 to each individual E:T tube containing different numbers of effector cells and carrying out the incubation step in a smaller volume to facilitate interactions, no inhibition of killing of K562 cells was detected. When this alternate assay and 99P006's IgG/IgG-ICs were used, NK cell killing against K562 cells increased from 8.81 to 10 $LU_{10}/10^6$ NK cells. Thus, addition of IgG and IgG-ICs to the NK cell lytic assay appeared to have no effect on killing of K562 cells.

DISCUSSION

As disease progresses during SIV infection of macaques, both viral load and SIV-specific antibody titers increase. In general, high antibody titers are correlated directly with high viral burdens; animals that are naturally slow progressors or those infected with attenuated strains have the lowest viral loads and antibody titers (31, 39). The exception occurs in those macaques that rapidly progress to AIDS and die in less than 6 months, in which case little or no detectable antibodies are generated despite high viral burdens (21, 31). In this report, as virus load and antibody titers increased in SIV-infected macaques, levels of circulating mIgG and/or IgG-ICs increased and bound CD16 on NK cells, with the result that, when whole blood was analyzed by flow cytometry, recognition of CD16 by MAb 3G8 was blocked, giving the erroneous perception that NK cells were being depleted. Generally, we did not observe actual decreases in numbers of NK cells in SIV-infected pigtailed macaques until late stages of infection, when the animals became lymphopenic and numbers of all lymphocyte subsets declined. The presence of increased levels of ICs in association with primate lentivirus-induced disease is not a new finding. Early in the AIDS epidemic, high levels of ICs were detected in HIV-infected individuals, and after the virus was identified as the etiologic agent of AIDS, these ICs were shown to contain HIV virions or proteins (36, 37, 51, 52, 54). Consistent with SIV infection of macaques, the formation of HIV-ICs was related to high titers of HIV-specific antibodies, high levels of HIV virion RNA in plasma, and progressive disease (14, 19, 51, 52, 54). Furthermore, complement fixation by HIV-ICs was shown to facilitate dissemination of virus bound as an IC to B cells, dendritic cells, or erythrocytes, thus contributing directly to infection of $CD4^+$ T cells and to disease (32, 36, 37, 53).

Many investigators use EDTA-treated whole blood to detect and quantify different types of leukocytes by flow cytometry; therefore, our observations are important and should be considered whenever a cell population is being evaluated by the presence or absence of any surface marker, not just CD16, that might be blocked by high concentrations of its natural ligand in blood. By using a whole-blood procedure, results similar to ours were obtained by Daniel et al. (14) and Mansour et al. (48), who detected decreased percentages and loss of absolute numbers of $CD16^+$ cells in blood samples from HIV-infected persons. They, however, did not attribute this putative cell loss to the possibility that ICs were blocking binding of the fluorochrome-labeled antibodies to CD16. These observations can explain some of the discrepancies that have been reported regarding the effect(s) of HIV or SIV infection on numbers of NK cells in susceptible hosts, especially if the MAb to CD16 recognizes an epitope on or near the Fc-binding region, like 3G8. Giavedoni et al. (29) used MAb 3G8 to evaluate $CD16^+$ $CD3^-$ NK cells in whole blood obtained from four rhesus macaques during the first 32 weeks after inoculation of SIVmac251; however, they did not observe progressive loss of these cells. Their result is easily explained because only one animal had elevated plasma $p27^{gag}$ levels and that animal had little or no

detectable antibodies to SIV structural proteins. Based on our results, both SIV-specific antibodies and a high level of viremia are required to block detection of CD16 by 3G8 in whole blood.

Although ICs can have a more detrimental effect physiologically than mIgG, the Fc portion of mIgG can bind to CD16, as shown by others (22, 23, 61), and contribute to decreases in MFI, such as we observed (Fig. 6 and 8). Similarly, ligation of CD16 by mIgG can lead to reversible functional defects in NK cell activity that are related both to direct cell killing and ADCC and to production of CC chemokines and cytokines, including IFN-γ (61, 62). However, in conjunction with other factors, such as costimulation signals, ligation of CD16 by mIgG can upregulate NK cell proliferation and cytokine release (61, 62). NK cell defects induced by mIgG binding to CD16 were reversed in the presence of added IFN-γ or interleukin-2 or if the incubation time of NK cells with mIgG was increased. Moreover, up- or downregulation of NK cell activity was dependent on the IgG1 subclass of mIgG (61).

In the context of lentivirus infections, decreased production of MIP-1α and -1β and RANTES might contribute to disease progression, because these CC chemokines can inhibit HIV/SIV infection of $CD4^+$ T cells that express the CCR5 coreceptor. It is difficult to determine the in vivo effects of mIgG and IC binding to CD16, but because (i) Engelhard et al. (23) showed that NK cell activity decreased in patients treated with gamma globulin and (ii) hypergammaglobulinemia is a hallmark of HIV infection (43), it is likely that circulating mIgG contributes to aberrant NK cell function in HIV-infected individuals. However, in numerous in vitro reconstruction experiments, in which various concentrations of purified IgG/IgG-ICs or macaque plasma samples containing ICs were added to enriched NK cells, we detected no inhibition of NK cell killing of K562 cells, consistent with a lack of inhibition of human NK cells by ICs (61). This finding was reproducible when enriched NK cells from either uninfected or SIV-infected macaque donors of the CD16-blocking antibodies and ICs were used. However, it is possible that SIV-ICs might inhibit NK activity in SIV-infected macaques. The question of whether, as SIV-ICs increase in infected macaques, other functional activities of NK cells, such as ADCC or IFN-γ production, are lost, the type and extent of any dysfunction, and its possible impact on disease progression are currently under investigation. Furthermore, a comprehensive analysis of the effects of SIV infection and high levels of ICs on expression of other NK receptors, which can be altered during HIV infection (27, 41), is needed. These include a complex array of activating and inhibitory receptors (e.g., NKG2A, NKG2D, NKp30, and NKp46), which are now being characterized in macaques (17, 49).

In summary, a consequence of high levels of HIV/SIV viremia and virus-specific antibodies is the formation of large numbers of HIV/SIV-ICs that can contribute to disease in several ways. The ICs can (i) fix and deplete complement components (57); (ii) bind to CD16, resulting in aberrant induction of cellular activation pathways and possible anergy (62, 67); (iii) facilitate dissemination of the virus as complement components attached to the HIV/SIV-ICs bind complement receptors on various cell types (32, 37, 51, 53); and (iv) mask recognition by CD16 of the Fc portions of antibodies bound to viral glycoproteins on infected cells, thereby inhibiting cell killing (61). Furthermore, the presence of large numbers of HIV/SIV-ICs could contribute to impairment of innate immune responses, such as decreased IFN-γ production (2), with secondary effects on transition to adaptive responses, leading to acquisition of opportunistic infections. Lastly, to develop a coherent picture of the effects of mIgG, ICs, and other host factors associated with HIV/SIV disease on NK cell numbers and functions, it is imperative that investigators reach a consensus regarding the immunophenotypes of subsets of this cell population in relevant species and be cognizant of factors that might yield results that are artifacts, such as those described here. Relative to detection of $CD16^+$ NK cells using whole-blood assay procedures, a possible solution is to employ a MAb, such as 214.1, that does not recognize the CD16 ligand-binding site (22).

ACKNOWLEDGMENTS

We thank Marion Spell for acquiring data on the FACSTAR and Michael Piatak and Jeffrey Lifson for comments on the manuscript and for quantification of SIV virion RNA in plasma samples.

This work was supported by Public Health Service grant AI49784 from the National Institutes of Health and was facilitated by the UAB Center for AIDS Research FACS core, NIH grant P30 AI027767.

REFERENCES

1. **Alter, G., J. M. Malenfant, R. M. Delabre, N. C. Burgett, X. G. Yu, M. Lichterfeld, J. Zaunders, and M. Altfeld.** 2004. Increased natural killer cell activity in viremic HIV-1 infection. J. Immunol. **173:**5305–5311.
2. **Azzoni, L., E. Papasavvas, J. Chehimi, J. R. Kostman, K. Mounzer, J. Ondercin, B. Perussia, and L. J. Montaner.** 2002. Sustained impairment of IFN-γ secretion in suppressed HIV-infected patients despite mature NK cell recovery: evidence for a defective reconstitution of innate immunity. J. Immunol. **168:**5764–5770.
3. **Azzoni, L., R. M. Rutstein, J. Chehimi, M. A. Farabaugh, A. Nowmos, and L. J. Montaner.** 2005. Dendritic and natural killer cell subsets associated with stable or declining $CD4^+$ cell counts in treated HIV-1-infected children. J. Infect. Dis. **191:**1451–1459.
4. **Banks, N. D., N. Kinsey, J. Clements, and J. E. K. Hildreth.** 2002. Sustained antibody-dependent cell-mediated cytotoxicity (ADCC) in SIV-infected macaques correlates with delayed progression to AIDS. AIDS Res. Hum. Retrovir. **18:**1197–1205.
5. **Baum, L. L., K. J. Cassutt, K. Knigge, R. Khattri, J. Margolick, C. Rinaldo, C. A. Kleeberger, P. Nishanian, D. R. Henrard, and J. Phair.** 1996. HIV-1 gp120-specific antibody-dependent cell-mediated cytotoxicity correlates with rate of disease progression. J. Immunol. **157:**2168–2173.
6. **Bernstein, H. B., A. L. Kinter, R. Jackson, and A. S. Fauci.** 2004. Neonatal natural killer cells produce chemokines and suppress HIV replication in vitro. AIDS Res. Hum. Retrovir. **20:**1189–1195.
7. **Biron, C. A., and L. Brossay.** 2001. NK cells and NKT cells in innate defense against viral infection. Curr. Opin. Immunol. **13:**458–464.
8. **Bryant, J., R. Day, T. L. Whiteside, and R. B. Herberman.** 1992. Calculation of lytic units for the expression of cell-mediated cytotoxicity. J. Immunol. Methods **146:**91–103.
9. **Carter, D. L., T. M. Shieh, R. L. Blosser, K. R. Chadwick, J. B. Margolick, J. E. K. Hildreth, J. E. Clements, and M. C. Zink.** 1999. CD56 identifies monocytes and not natural killer cells in rhesus macaques. Cytometry **37:**41–50.
10. **Carver, F. M., and J. M. Thomas.** 1988. Natural killer cells in rhesus monkeys: properties of effector cells which lyse Raji targets. Cell. Immunol. **117:**56–69.
11. **Cerwenka, A., and L. L. Lanier.** 2001. Natural killer cells, viruses and cancer. Nat. Rev. Immunol. **1:**41–49.
12. **Chang, L., G. A. Gusewitch, D. B. W. Chritton, J. C. Folz, L. K. Lebeck, and S. L. Nehlsen-Cannarella.** 1993. Rapid flow cytometric assay for the assessment of natural killer cell activity. J. Immunol. Methods **166:**45–54.
13. **Connick, E., D. G. Marr, X.-Q. Zhang, S. J. Clark, M. S. Saag, R. T. Schooley, and T. J. Curiel.** 1996. HIV-specific cellular and humoral immune responses in primary HIV infection. AIDS Res. Hum. Retrovir. **12:**1129–1140.
14. **Daniel, V., C. Susal, R. Weimer, R. Zimmermann, A. Huth-Kuhne, and G. Opelz.** 2001. Association of immune complexes and plasma viral load with $CD4^+$ cell depletion, $CD8^+$ DR^+ and $CD16^+$ cell counts in HIV^+ hemophilia patients. Implications for the immunopathogenesis of HIV-induced $CD4^+$ lymphocyte depletion. Immunol. Lett. **76:**69–78.
15. **De Boer, R. J., H. Mohri, D. D. Ho, and A. S. Perelson.** 2003. Turnover rates

of B cells, T cells, and NK cells in simian immunodeficiency virus-infected and uninfected rhesus macaques. J. Immunol. **170:**2479–2487.

16. **Degli-Esposti, M. A., and M. J. Smyth.** 2005. Close encounters of different kinds: dendritic cells and NK cells take centre stage. Nat. Rev. Immunol. **5:**112–124.
17. **De Maria, A., R. Biassoni, M. Fogli, M. Rizzi, C. Cantoni, P. Costa, R. Conte, D. Mavilio, B. Ensoli, A. Cafaro, A. Moretta, and L. Moretta.** 2001. Identification, molecular cloning and functional characterization of NKp46 and NKp30 natural cytotoxicity receptors in *Macaca fascicularis* NK cells. Eur. J. Immunol. **31:**3546–3556.
18. **Desrosiers, R. C.** 1992. HIV with multiple gene deletions as a live attenuated vaccine for AIDS. AIDS Res. Hum. Retrovir. **8:**411–421.
19. **Dianzani, F., G. Antonelli, E. Riva, O. Turriziani, L. Antonelli, S. Tyring, D. A. Carrasco, H. Lee, D. Nguyen, J. Pan, J. Poast, M. Cloyd, and S. Baron.** 2002. Is human immunodeficiency virus RNA load composed of neutralized immune complexes? J. Infect. Dis. **185:**1051–1054.
20. **Douglas, S. D., S. J. Durako, N. B. Tustin, J. Houser, L. Muenz, S. E. Starr, and C. Wilson for the Adolescent Medicine HIV/AIDS Research Network.** 2001. Natural killer cell enumeration and function in HIV-infected and high-risk uninfected adolescents. AIDS Res. Hum. Retrovir. **17:**543–552.
21. **Dykhuizen, M., J. L. Mitchen, D. C. Montefiori, J. Thomson, L. Acker, H. Lardy, and C. D. Pauza.** 1998. Determinants of disease in the simian immunodeficiency virus-infected rhesus macaque: characterizing animals with low antibody responses and rapid progression. J. Gen. Virol. **79:**2461–2467.
22. **Edberg, J. C., and R. P. Kimberly.** 1997. Cell type-specific glycoforms of FcγRIIIa (CD16). J. Immunol. **159:**3849–3857.
23. **Engelhard, D., J. L. Waner, N. Kapoor, and R. A. Good.** 1986. Effect of intravenous immune globulin on natural killer cell activity: possible association with autoimmune neutropenia and idiopathic thrombocytopenia. J. Pediatr. **108:**77–81.
24. **Fehniger, T. A., G. Herbein, H. Yu, M. I. Para, Z. P. Bernstein, W. A. O'Brien, and M. A. Caligiuri.** 1998. Natural killer cells from HIV-1$^+$ patients produce C-C chemokines and inhibit HIV-1 infection. J. Immunol. **161:** 6433–6438.
25. **Forthal, D. N., G. Landucci, and E. S. Daar.** 2001. Antibody from patients with acute human immunodeficiency virus (HIV) infection inhibits primary strains of HIV type 1 in the presence of natural-killer effector cells. J. Virol. **75:**6953–6961.
26. **Fultz, P. N., P. J. Vance, M. J. Endres, B. Tao, J. D. Dvorin, I. C. Davis, J. D. Lifson, D. C. Montefiori, M. Marsh, M. H. Malim, and J. A. Hoxie.** 2001. In vivo attenuation of simian immunodeficiency virus by disruption of a tyrosine-dependent sorting signal in the envelope glycoprotein cytoplasmic tail. J. Virol. **75:**278–291.
27. **Galiani, M. D., E. Aguardo, R. Tarazona, P. Romero, I. Molina, M. Santamaria, R. Solana, and J. Pena.** 1999. Expression of killer inhibitory receptors on cytotoxic cells from HIV-1-infected individuals. Clin. Exp. Immunol. **115:**472–476.
28. **Gerosa, F., A. Gobbi, P. Zorzi, S. Burg, F. Briere, G. Carra, and G. Trinchieri.** 2005. The reciprocal interaction of NK cells with plasmacytoid or myeloid dendritic cells profoundly affects innate resistance functions. J. Immunol. **174:** 727–734.
29. **Giavedoni, L. D., M. C. Velasquillo, L. M. Parodi, G. B. Hubbard, and V. L. Hodara.** 2000. Cytokine expression, natural killer cell activation, and phenotypic changes in lymphoid cells from rhesus macaques during acute infection with pathogenic simian immunodeficiency virus. J. Virol. **74:**1648–1657.
30. **Gomez-Roman, V. R., L. J. Patterson, D. Venzon, D. Liewehr, K. Aldrich, R. Florese, and M. Robert-Guroff.** 2005. Vaccine-elicited antibodies mediate antibody-dependent cellular cytotoxicity correlated with significantly reduced acute viremia in rhesus macaques challenged with SIV_{mac251}. J. Immunol. **174:**2185–2189.
31. **Hirsch, V. M., T. R. Fuerst, G. Sutter, M. W. Carroll, L. C. Yang, S. Goldstein, M. Piatak, Jr., W. R. Elkins, W. G. Alvord, D. C. Montefiori, B. Moss, and J. D. Lifson.** 1996. Patterns of viral replication correlate with outcome in simian immunodeficiency virus (SIV)-infected macaques: effect of prior immunization with a trivalent SIV vaccine in modified vaccinia virus Ankara. J. Virol. **70:**3741–3752.
32. **Horakova, E., O. Gasser, S. Sadallah, J. M. Inal, G. Bourgeois, I. Ziekau, T. Klimkait, and J. A. Schifferli.** 2004. Complement mediates the binding of HIV to erythrocytes. J. Immunol. **173:**4236–4241.
33. **Hu, P.-F., L. E. Hultin, P. Hultin, M. A. Hausner, K. Hirji, A. Jewett, B. Bonavida, R. Detels, and J. V. Giorgi.** 1995. Natural killer cell immunodeficiency in HIV disease is manifest by profoundly decreased numbers of CD16$^+$ CD56$^+$ cells and expansion of a population of CD16^{dim} CD56$^-$ cells with low lytic activity. J. Acquir. Immune Defic. Syndr. **10:**331–340.
34. **Ibegbu, C., A. Brodie-Hill, A. P. Kourtis, A. Carter, H. McClure, Z. Wei Chen, and A. J. Nahmias.** 2001. Use of human CD3 monoclonal antibody for accurate CD4$^+$ and CD8$^+$ lymphocyte determinations in macaques: phenotypic characterization of the CD3$^-$ CD8$^+$ cell subset. J. Med. Primatol. **30:**291–298.
35. **Ironson, G., E. Balbin, G. Solomon, J. Fahey, N. Klimas, N. Schneiderman, and M. A. Fletcher.** 2001. Relative preservation of natural killer cell cytotoxicity and number in healthy AIDS patients with low CD4 cell counts. AIDS **15:**2065–2073.
36. **Jakubik, J. J., M. Saifuddin, D. M. Takefman, and G. T. Spear.** 1999. B lymphocytes in lymph nodes and peripheral blood are important for binding immune complexes containing HIV-1. Immunology **96:**612–619.
37. **Jakubik, J. J., M. Saifuddin, D. M. Takefman, and G. T. Spear.** 2000. Immune complexes containing human immunodeficiency virus type 1 primary isolates bind to lymphoid tissue B lymphocytes and are infectious for T lymphocytes. J. Virol. **74:**552–555.
38. **Johann, S., G. Blumel, M. Lipp, and R. Forster.** 1995. A versatile flow cytometry-based assay for the determination of short- and long-term natural killer cell activity. J. Immunol. Methods **185:**209–216.
39. **Kestler, H., T. Kodama, D. Ringler, M. Marthas, N. Pedersen, A. Lackner, D. Regier, P. Sehgal, M. Daniel, N. King, and R. Desrosiers.** 1990. Induction of AIDS in rhesus monkeys by molecularly cloned simian immunodeficiency virus. Science **248:**1109–1112.
40. **Kottilil, S., T.-W. Chun, S. Moir, S. Liu, M. McLaughlin, C. W. Hallahan, F. Maldarelli, L. Corey, and A. S. Fauci.** 2003. Innate immunity in human immunodeficiency virus infection: effect of viremia on natural killer cell function. J. Infect. Dis. **187:**1038–1045.
41. **Kottilil, S., K. Shin, M. Planta, M. McLaughlin, C. W. Hallahan, M. Ghany, T.-W. Chun, M. C. Sneller, and A. S. Fauci.** 2004. Expression of chemokine and inhibitory receptors on natural killer cells: effect of immune activation and HIV viremia. J. Infect. Dis. **189:**1193–1198.
42. **LaBranche, C. C., M. M. Sauter, B. S. Haggarty, P. J. Vance, J. Romano, T. K. Hart, P. J. Bugelski, M. Marsh, and J. A. Hoxie.** 1995. A single amino acid change in the cytoplasmic domain of the simian immunodeficiency virus transmembrane molecule increases envelope glycoprotein expression on infected cells. J. Virol. **69:**5217–5227.
43. **Lane, H. C., H. Masur, L. C. Edgar, G. Whalen, A. H. Rook, and A. S. Fauci.** 1983. Abnormalities of B-cell activation and immunoregulation in patients with the acquired immunodeficiency syndrome. N. Engl. J. Med. **309:**453–458.
44. **Lanier, L. L., G. Yu, and J. H. Phillips.** 1991. Analysis of FcγRIII (CD16) membrane expression and association with CD3ζ and FcεRI-γ by site-directed mutation. J. Immunol. **146:**1571–1576.
45. **Leibson, P. J.** 1997. Signal transduction during natural killer cell activation: inside the mind of a killer. Immunity **6:**655–661.
46. **Lifson, J. D., J. L. Rossio, M. Piatak, Jr., T. Parks, L. Li, R. Kiser, V. Coalter, B. Fisher, B. M. Flynn, S. Czajak, V. M. Hirsch, K. A. Reimann, J. E. Schmitz, J. Ghrayeb, N. Bischofberger, M. A. Nowak, R. C. Desrosiers, and D. Wodarz.** 2001. Role of CD8$^+$ lymphocytes in control of simian immunodeficiency virus infection and resistance to rechallenge after transient early antiretroviral treatment. J. Virol. **75:**10187–10199.
47. **Lucia, B., C. Jennings, R. Cauda, L. Ortona, and A. L. Landay.** 1995. Evidence of a selective depletion of a CD16$^+$ CD56$^+$ CD8$^+$ natural killer cell subset during HIV infection. Cytometry **22:**10–15.
48. **Mansour, I., C. Doinel, and P. Rouger.** 1990. CD16$^+$ NK cells decrease in all stages of HIV infection through a selective depletion of the CD16$^+$ CD8$^+$ CD3$^-$ subset. AIDS Res. Hum. Retrovir. **6:**1451–1457.
49. **Mavilio, D., J. Benjamin, D. Kim, G. Lombardo, M. Daucher, A. Kinter, E. Nies-Kraske, E. Marcenaro, A. Moretta, and A. S. Fauci.** 2005. Identification of NKG2A and NKp80 as specific natural killer markers in rhesus and pig-tailed monkeys. Blood **106:**1718–1725.
50. **Mavilio, D., G. Lombardo, J. Benjamin, D. Kim, D. Follman, E. Marcenaro, M. A. O'Shea, A. Kinter, C. Kovacs, A. Moretta, and A. S. Fauci.** 2005. Characterization of CD56$^-$/CD16$^+$ natural killer (NK) cells: a highly dysfunctional NK subset expanded in HIV-infected viremic individuals. Proc. Natl. Acad. Sci. USA **102:**2886–2889.
51. **McDougal, J. S., M. Hubbard, J. K. A. Nicholson, B. M. Jones, R. C. Holman, J. Roberts, D. B. Fishbein, H. W. Jaffe, J. E. Kaplan, T. J. Spira, and B. L. Evatt.** 1985. Immune complexes in the acquired immunodeficiency syndrome (AIDS): relationship to disease manifestation, risk group, and immunologic defect. J. Clin. Immunol. **5:**130–138.
52. **McHugh, T. M., D. P. Stites, M. P. Busch, J. F. Krowka, R. B. Stricker, and H. Hollander.** 1988. Relation of circulating levels of human immunodeficiency virus (HIV) antigen, antibody to p24, and HIV-containing immune complexes in HIV-infected patients. J. Infect. Dis. **158:**1088–1091.
53. **Moir, S., A. Malaspina, Y. Li, T.-W. Chun, T. Lowe, J. Adelsberger, M. Baseler, L. A. Ehler, S. Liu, R. T. Davey, J. M. Mican, and A. S. Fauci.** 2000. B cells of HIV-1-infected patients bind virions through CD21-complement interactions and transmit infectious virus to activated T cells. J. Exp. Med. **192:**637–645.
54. **Morrow, W. J. W., M. Wharton, R. B. Stricker, and J. A. Levy.** 1986. Circulating immune complexes in patients with acquired immune deficiency syndrome contain the AIDS-associated retrovirus. Clin. Immunol. Immunopathol. **40:**515–524.
55. **Oliva, A., A. L. Kinter, M. Vaccarezza, A. Rubbert, A. Catanzaro, S. Moir, J. Monaco, L. Ehler, S. Mizell, R. Jackson, Y. Li, J. W. Romano, and A. S. Fauci.** 1998. Natural killer cells from human immunodeficiency virus (HIV)-infected individuals are an important source of CC-chemokines and suppress HIV-1 entry and replication in vitro. J. Clin. Investig. **102:**223–231.

56. **Ortaldo, J. R., A. T. Mason, and J. J. O'Shea.** 1995. Receptor-induced death in human natural killer cells: involvement of CD16. J. Exp. Med. **181:**339–344.
57. **Peng, X.-X., M. A. Wainberg, Y. Tao, and B. G. Brenner.** 1996. Immunoglobulin and complement complexes in blood following infection with human immunodeficiency virus type 1. Clin. Diagn. Lab. Immunol. **3:**128–131.
58. **Rabinowich, H., L. Pricop, R. B. Herberman, and T. L. Whiteside.** 1994. Expression and function of CD7 molecule on human natural killer cells. J. Immunol. **152:**517–526.
59. **Scott-Algara, D., L. X. Truong, P. Versmisse, A. David, T. T. Luong, N. V. Nguyen, I. Theodorou, F. Barre-Sinoussi, and G. Pancino.** 2003. Increased NK cell activity in HIV-1-exposed but uninfected Vietnamese intravascular drug users. J. Immunol. **171:**5663–5667.
60. **Slukvin, I. I., D. I. Watkins, and T. G. Golos.** 2001. Phenotypic and functional characterization of rhesus monkey decidual lymphocytes: rhesus decidual large granular lymphocytes express CD56 and have cytolytic activity. J. Reprod. Immunol. **50:**57–79.
61. **Sulica, A., C. Galatiuc, M. Manciulea, A. C. Bancu, A. C. DeLeo, T. L. Whiteside, and R. B. Herberman.** 1993. Regulation of human natural cytotoxicity by IgG. IV. Association between binding of monomeric IgG to the Fc receptors on large granular lymphocytes and inhibition of natural killer (NK) cell activity. Cell. Immunol. **147:**397–410.
62. **Sulica, A., D. Metes, M. Gherman, T. L. Whiteside, and R. B. Herberman.** 1996. Divergent effects of FcγRIIIA ligands on the functional activities of human natural killer cells in vitro. Eur. J. Immunol. **26:**1199–1203.
63. **Tamm, A., and R. E. Schmidt.** 1996. The binding epitopes of human CD16 (FcγRIII) monoclonal antibodies. Implications for ligand binding. J. Immunol. **157:**1576–1581.
64. **Tanneau, F., M. McChesney, O. Lopez, P. Sansonetti, L. Montagnier, and Y. Riviere.** 1990. Primary cytotoxicity against the envelope glycoprotein of human immunodeficiency virus-1: evidence for antibody-dependent cellular cytotoxicity in vivo. J. Infect. Dis. **162:**837–843.
65. **Ullum, H., P. C. Gotzsche, J. Victor, E. Dickmeiss, P. Skinhoj, and B. K. Pedersen.** 1995. Defective natural immunity: an early manifestation of human immunodeficiency virus infection. J. Exp. Med. **182:**789–799.
66. **Walzer, T., M. Dalod, S. H. Robbins, L. Zitvogel, and E. Vivier.** 2005. Natural-killer cells and dendritic cells: "l'union fait la force". Blood **106:**2252–2258.
67. **Warren, H. S., and B. F. Kinnear.** 1999. Quantitative analysis of the effect of CD16 ligation on human NK cell proliferation. J. Immunol. **162:**735–742.
68. **Webster, R. L., and R. P. Johnson.** 2005. Delineation of multiple subpopulations of natural killer cells in rhesus macaques. Immunology **115:**206–214.
69. **Wu, J., J. C. Edberg, P. B. Redecha, V. Bansal, P. M. Guyre, K. Coleman, J. E. Salmon, and R. P. Kimberly.** 1997. A novel polymorphism of FcγRIIIa (CD16) alters receptor function and predisposes to autoimmune disease. J. Clin. Investig. **100:**1059–1070.